

Phosphate Recovery from Real Fresh Urine by Mg/Fe Treated Natural Bentonite Clay

Michael Biney¹, Swati Chandola², Vipin Kumar Saini³

Materials and Environmental Chemistry Research Laboratory,

School of Environment & Natural Resources, Doon University, Dehradun, Uttarakhand, 248001, India

Abstract:- The study aimed to modify Bentonite Clay into a composite adsorbent (BENR 2:8) through Mg/Fe pillaring. The modification process involved the removal of residual cationic species from the Bentonite Clay, which increased its surface negative charge. This, in turn, facilitated faster and higher adsorption of BENR 2:8 compared to raw, un-pillared Bentonite Clay. According to the kinetics study, the selected BENR 2:8 follows Elovich isotherm expression, and the rate of solute adsorption decreases exponentially as the amount of adsorbed solute increases. The adsorption mechanism is explained by surface chemistry changes and adsorption kinetics. Notably, BENR 2:8 has a higher maximum phosphate adsorption (up to 22.03%) than raw Bentonite Clay (up to 2.68%).

Keywords:- Bentonite, Phosphorus, Adsorption, Pillared Clay, Urine, Resource recovery.

I. INTRODUCTION

Phosphorus (P) is the 12th most abundant element in the Earth's crust and is an essential nutrient for all types of living organisms. In natural and waste waters, phosphorus occurs mainly as dissolved phosphate, making it the most common form of phosphorus present in natural waters. Phosphate (PO_4) is found in all biological organisms and is assumed as a basic part of the development of cell membranes and cell walls (in plants), DNA, cellular energy, and many others. Despite its abundance, the availability of phosphorus for future generations is uncertain since it is a non-renewable mineral. Most of its supply comes from the mining of 'phosphate rock's, which serves as the only existing reserves of the earth's crust and is widely used as fertilizer. Unfortunately, these reserves of phosphate rock are estimated to be depleted within the next century (Cordell et al., 2009; Farmer, 2018; Genz et al., 2004). Naturally, the phosphorus stream follows a progression of biogeochemical processes involving both mechanical transference and physical, chemical, as well as biological transformations. Thus, the natural phosphorus flow takes longer due to its slow occurrences (one single loop of these could take over a million years), making it relatively constant in quantity with a closed loop.

The flow of phosphorus in the natural environment happens in three cycles. The first is the inorganic cycle, which is related to phosphorus in the crust of the earth. For a long time, the phosphorus travels through the inorganic process, beginning with the stones, which gradually disintegrate with climate and are added to soil, from which the phosphorus is steadily filtered from the land into waterways and forward to the ocean, where it, in the end,

form insoluble calcium phosphate and sinks to the ocean bottom as dregs (Folmi 1996). It stays there till it regenerates to new sedimentary rock subsequently of geographic pressure. On a timescale of many years, these sediments' area unit elates to make a new earth. Thus, the rock area unit is weathered and this completes the inorganic cycle (Schlesinger 1991). Practically, all the phosphorus, present on earth, is derived from the weathering of calcium phosphate minerals, specifically apatite [$\text{Ca}_5(\text{PO}_4)_3\text{OH}$]. Approximately, 13MMT P/yr. of this calcium phosphate is released to form soils annually (Emsley 2000).

The second phosphorous cycle is the organic cycle which moves phosphorus through living organic entities as some portion of the food chain. These are a land-based phosphorus cycle that transfers phosphorus from soil to plants, to creatures, and back to soil again. It is a water-based organic cycle that flows phosphorus among the creatures living in waterways, lakes, and oceans. Estimates by Emsley (1980), Meybreck (1982), Richey (1983), and Filippelli (2002) suggest that the amount of phosphorus worldwide ranges from 19×10^3 to 200×10^3 MMT P. However, despite its abundance in the soil, only a small amount of phosphorus is made available to biota. The available phosphorus pool is estimated to contain about 1,805 to 3,000 MMT P (Grove 1992), with Emsley (1980) and Richey (1983) suggesting a most likely range of 2,000 to 2,600 MMT P. A considerable amount of phosphorus, between 27106 to 840106 MMT P, can be found in the oceans, with seawater containing about 80103 to 120103 MMT P and the rest accumulating in sediments (Emsley 1980; Richey 1983; Grove 1992; Filippelli 2002; Smil 2002). The societal cycle is the final cycle in the three different phosphate cycle that consider global phosphate consumption. In this cycle, the phosphate rock is at first changed over to phosphoric acid (P_2O_5) by reacting with sulfuric acid (Villalba et al. 2008). The phosphoric acid is then further processed to produce fertilizers, food-grade and feed-grade additives, and detergents. According to a report by the Food and Agriculture Organization (FAO), the worldwide utilization of all phosphate fertilizers surpassed 1MMT P/yr. during the last part of the 1930s. After arriving at 14.8 MMT P/yr. in 1980, the world utilization of phosphate fertilizers has been generally steady. It was 14.8 MMT P (34 MMT P_2O_5) in the factual year 2002 – 2003, and it somewhat diminished to 13.8 MMT P (31.5 MMT P_2O_5) in the measurable year 2003 – 2004 (FAO 2005) which generally represented 78% of the global production of phosphorus from phosphate rock. China is the world's top fertilizer processing country contributing 22% and 28% respectively, to world production and utilization; the main three economies (China, the United States, and India)

accounted for one-half of the world's phosphorous consumption.

Municipal wastewater may contain 4 to 16 mg/L of phosphorus as P (Metcalf & Eddy, 2003). Fundamentally, the standard types of phosphorus found in the aqueous solution include orthophosphate, polyphosphate, and organic phosphate. The orthophosphates are accessible for biological metabolism without further breakdown. Polyphosphates include those molecules with at least two or more phosphorus atoms, oxygen atoms, and, at times, hydrogen atoms consolidated in a complex molecule. The polyphosphate goes through hydrolysis in an aqueous solution and returns to the orthophosphate structure, notwithstanding, this hydrolysis is normally slow. However, the organically bound phosphorus is mostly of minor significance in most domestic wastes but is a huge part of industrial wastes and wastewater sludges (Metcalf & Eddy, 2003). Surface and groundwater may often be contaminated by both natural and anthropogenic sources of phosphates. Natural sources of phosphorus in both surface and groundwater include atmospheric deposition, regular disintegration of rocks and minerals, weathering of soluble inorganic materials, rotting biomass, overflow, and sedimentation. Anthropogenic sources incorporate; fertilizers and compost, wastewater and septic framework gushing, animal wastes, detergents, industrial discharge, phosphate mining, drinking water treatment, forest fires, and synthetic material development (Sprail T.B et al, 1998; Sheila Murphy, 2005; Mueller D.K et al 1995; Manahan S.E, 1993). Excessive levels of phosphates in water bodies generally prompt eutrophication, a condition of accelerated living aquatic-based organisms (algae) in water bodies that results in oxygen depletion, which can destroy an aquatic ecosystem. These excessive algae on the water surfaces can lead to scum which may result in clogged pipelines, cause a foul odour when decay, as well as restrict recreational activities on water bodies (Mueller D.K et al. 1995). Furthermore, algae blooms have resulted in related health issues including skin irritation and even death to both humans and animals depending on the type and duration of exposure (Brain Oram, 2005).

II. MATERIALS AND METHODS

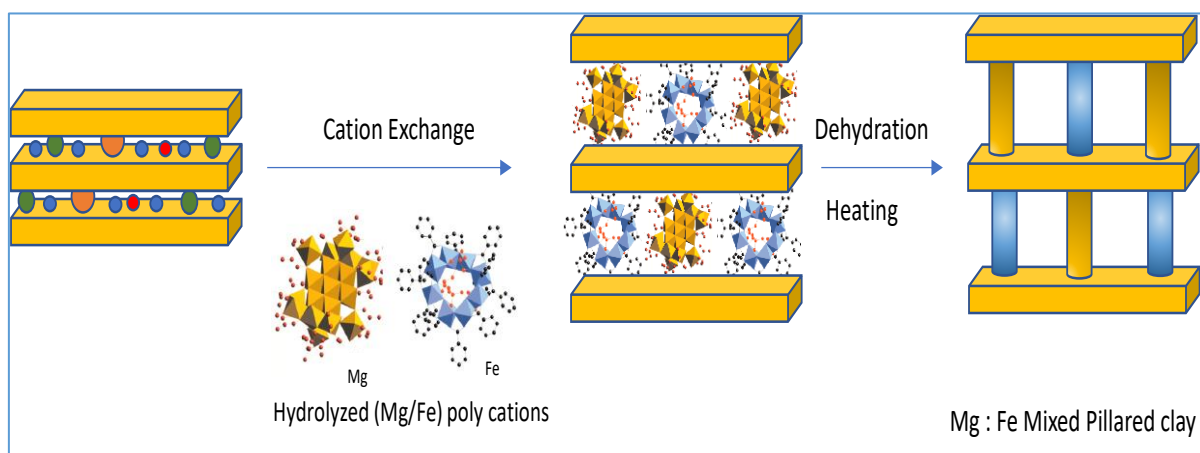
A. Materials

The natural clay used in this study originated from the mines of Rajasthan. The sample was graciously provided by Neelkanth Chemical & Mineral Ltd (Jodhpur, Rajasthan). The sample is commercialized by the manufacturer as Bentonite, which contains >85% of Montmorillonite as its principal clay mineral. Due to its origin, the sample was referred to as BENR in this study. Ammonium Acetate (NH_4AcO , $\geq 98\%$) extra pure AR (SRL), Potassium Phosphate Dihydrogen Orthophosphate (KHPO_4 , $\geq 99.5\%$) monobasic extra pure AR, Antimony Potassium Tartrate Trihydrate ($\text{C}_8\text{H}_4\text{K}_2\text{O}_{12}\text{Sb}_2 \cdot 3\text{H}_2\text{O}$ $\geq 99.0\%$) extra pure AR, and Ascorbic Acid ($\text{C}_6\text{H}_8\text{O}_6$ $\geq 99.5\%$) extra pure AR were supplied by Rankem. Ammonium Heptamolybdate Tetrahydrate ($(\text{NH}_4)_6\text{Mo}_7\text{O}_{24}$ $\geq 99.0\%$) was supplied by Emplura. Ammonium Sulfate ($(\text{NH}_4)_2\text{SO}_4$, $\geq 99.0\%$) was

supplied by Rankem, Sodium Hypochlorite solution of approximately 4% w/v available chlorine was supplied by Merck, Sodium Nitroprusside Dihydrate ($\text{Na}_2[\text{Fe}(\text{CN})_5\text{NO}] \cdot 2\text{H}_2\text{O}$ $\geq 99.0\%$) was supplied by Merck Life Science Ltd - India, Manganese (II) Sulphate ($\text{MnSO}_4 \cdot \text{H}_2\text{O}$ ≥ 98.0) monohydrate was supplied by Central Drug House (P) Ltd., Iron (III) Chloride Anhydrous (FeCl_3 $\geq 98.0\%$) was supplied by Emplura, Magnesium Sulphate Heptahydrate ($\text{MgSO}_4 \cdot 7\text{H}_2\text{O}$ $\geq 99.0\%$) was supplied by RFCL Limited (India). During the entire experimental study, the dilution and final washings were conducted with Milli-Q water.

B. Synthesis of Mg/Fe PILC

The Mg/Fe PILC was prepared by following the methods in the literature with some modifications. Firstly, different ratios of Mg/Fe metal solution of 2.5 mmol/g of clay were prepared in an RBF with 25mL of double-distilled water. It was heated on a magnetic stirrer to 80°C and the same temperature was maintained throughout the process. Then 10mmol of NaOH solution was added dropwise and allowed to reflux for 2 h. The solution was allowed to age for the next 24 h. Afterward, 2g of Raw bentonite (BENR) was dispersed in 50mL double distilled water, and the aged Mg/Fe solution was added to it dropwise at 80°C with continuous stirring. The suspension was refluxed for 2 h and left to age for the next 24 h. The aged clay was centrifuged and washed with a double-distilled water dialysis tube (Sigma-Aldrich, Dialysis tubing cellulose membrane avg. flat width 33mm (1.3)). The water around the dialysis tube was changed twice daily until TDS < 1 is obtained. Thereafter, the clay was separated and heated in air at 60°C for 24 h. The dried samples were then heated at 110°C for another 24 h. The dried samples were then heated at 110°C for another 24 h. The samples were labelled and stored for further use. For the above synthesis, samples of variable Mg/Fe ratio were prepared, where the ratio of Mg/Fe was varied as 0:10, 1:9, 2:8, 3:7, 4:6, 5:5, 6:4, 7:3, 8:2, 9:1, 10:0 and the samples were named accordingly. For example, BENR 1:9 involves 0.25mmol of Mg: 2.25mmol of Fe in 1g of clay.



Scheme 1: Preparation of Bentonite Pillared Clay

C. Characterization

The surface chemistry of the Mg/Fe PILC adsorbent before and after treatment was studied. Fourier transform infrared spectroscopy (FTIR) (SHIMADZU CORP. 01228) was used to study its reactive groups with the range of 500-4000 cm^{-1} . It is evident from the spectra that the surface chemistry of natural clay BENR (0:0) starts changing as it moves to BENR (0:10). The change in the relative concentration of both Mg and Fe in the samples leads to differences in structural chemistry. Some of the FTIR bands did not change throughout the samples, which indicates that the 2:1 aluminosilicate layer of MMT did not get affected during the pillaring process and the modification took place only in the interlayer space. Various concentration of Fe and Mg, in samples leads to the formation of different sizes of poly-hydroxy cations of these metals, which replaced the existing cations in the interlayer space of the clay. After aging and thermal treatment these poly-hydroxy cations, get dehydrated and converts into stable metal oxide pillars. This process gives rise to an increase in basal spacing in the material, according to the size of polycationic species, and also moderation in surface chemistry as per the chemical properties (acidity) of the metal ions involved.

D. Adsorption Experiment

The batch experiments were examined in an Erlenmeyer flask by adding a known amount of the prepared PILC material (0.1g) into 50 mL of Potassium Phosphate solution containing 10 ppm of phosphate ions. The reaction contents were rotated in a magnetic water bath at a rotation speed of 150 rpm at a fixed room temperature for 24h. After adsorption, the absorbance of phosphate concentration was analyzed using UV-spectrophotometer (Thermo Fisher Scientific –Shanghai, Evolution 201 model) in all 11 PILC samples.

For the determination of phosphate in an aqueous sample, Molybdenum blue colorimetric method (APHA 1995) was used on a UV-spectrophotometer (Evolution 201 model). In summary, different standards were prepared from a stock solution of Phosphate solution (using KH_2PO_4) and placed in a volumetric flask. A blank solution of known volume was also included. A known volume of combined reagent (which consists of 2.5M H_2SO_4 , Potassium Antimony Tartrate, Ammonium Molybdate, and Ascorbic

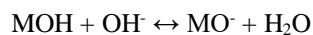
acid) was added to each analytical solution, shaken thoroughly, and made up to the mark on the volumetric flask with Milli-Qwater. The analytical solution was then allowed 45 mins for color development. The amount of adsorption was computed with the following equation,

$$q_e = \frac{C_0 - C_e}{w} \times V \quad (1)$$

Here q_e is the amount of adsorption in $\text{mg}\cdot\text{g}^{-1}$ the C_0 and C_e are the initial and equilibrium concentrations of the solution in $\text{mg}\cdot\text{L}^{-1}$, and 'w' is the mass of the adsorbents (g), and V is the volume of solution (L).

E. Desorption Experiment

The regeneration of exhausted adsorbent material was investigated as a function of desorbing solution (NaOH) concentration. In this study, the commonly utilized desorption method through sodium hydroxide was used. Desorption of adsorbed phosphate on the PILC material (BENR 2:8) by NaOH solution is actually the inverse of adsorption. Therefore, it was conceivable that a high NaOH concentration and a low phosphate concentration due to the high liquid ratio facilitated the desorption process. Basically, phosphate totally exists as PO_4^{3-} in NaOH solution but the hydroxyl groups might experience further deprotonation according to:



This reaction results in the formation of a negatively charged surface which after desorption was however not advantageous for phosphate capture. Hence to restore the reactivity of the hydroxyl groups, it was essential to regain the protonated status by acidification to a lower pH. Therefore, after the phosphate adsorption, the NaOH solution whose concentration varied from 0.1 to 2M was added as the desorption agent to generate. The flasks were shaken at 20°C at a speed of 300rpm in a water bath. After 24 h, the suspension was centrifuged, the phosphate concentration in the supernatant was measured, and the amount of phosphate desorbed from BENR 2:8 (q_d) was calculated as follows:

$$q_d = \frac{C_d \cdot V}{m} \quad (2)$$

Desorption efficiency was calculated using the following equation:

$$(\eta) = \frac{q_d}{q_e} * 100\% \quad (3)$$

Where C_d is the P concentration in the supernatant after the desorption step (mg/L), V is the volume of NaOH solution added as the desorption reagent (L), and q_e is the amount of phosphate adsorbed (mg/g). In the study, it was realized that NaOH 2M exhibited the highest desorption capacity similar to other literature reviews. Therefore, further desorption studies were conducted in NaOH 2M solution.

F. Experimental data validation

The adsorption and desorption tests were conducted three times, and the mean values were reported. The errors related to the experimental process, which includes the measurement of initial or equilibrium concentration, solution volume, and adsorbent mass, were estimated from method replications and are presented with vertical error bars.

III. RESULTS AND DISCUSSION

A. Characterization of nanotextural properties

The FTIR image of the Bentonite clay and its pillared samples were recorded (in the 4000-500 cm^{-1} range) and presented in Figure 1. The spectral band of high wavenumber between 3350 - 3700 cm^{-1} represents the presence of water molecules in interlayers of these samples. Here a symmetric O-H stretching vibrations for H-bonded water can be observed at 3450 cm^{-1} . A band at a higher wavenumber in samples indicates the presence of structural OH groups, coordinated with Al atoms of the octahedral layer, which disappeared in the pillared clays. In pillared clay samples, an additional band near 3652 cm^{-1} is observed due to a change in the position of the Si-OH group in the structure of samples. The OH bending vibration band in samples at 1653 cm^{-1} is shifted to lower wavenumbers in pillared clays due to the intercalation of metal-polyoxocations. The band at 1122 cm^{-1} , in samples which is due to Si-O stretching (out of plane), also shifted to a lower wavenumber after pillaring. A strong band at 984 cm^{-1} is attributed to Si-O-Si stretching vibrations in the tetrahedral structure of the clay layer. This band shifted to a lower wavenumber as the amount of Mg increased (980 cm^{-1}) but remains unchanged in the last two samples. Similarly, no change in Mg-Al-OH bending (917

cm^{-1}) is observed after pillaring whereas, in BENR2: Several low-intensity bands can be observed between 550 cm^{-1} and 1000 cm^{-1} that are attributed to Mg-O and Fe-O, stretching caused by pillaring which also confirms the success of the pillaring.

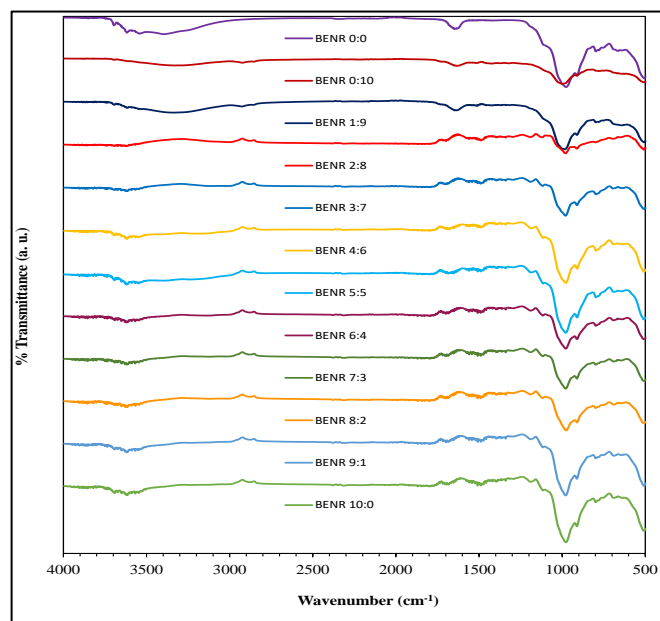


Fig. 1: FTIR spectra of BENR 2:8 and Raw unpillared bentonite and modified bentonite with various ratios of Mg:Fe

When a material surface comes into contact with an aqueous solution, the charge it acquires depends on the solution's pH. This charge is observed through the point of zero charges (pHzpc) of the material. The pHzpc is the pH at which the material's surface charge is neutralized by OH⁻ or H⁺ ions from the solution. The pHzpc value can be used to compare the surface behavior of materials. For instance, if the pH is less than pHzpc, the material's surface will have a positive charge, and vice-versa.

In the case of BENR 2:8, the observed pHzpc value is 3.2 (Figure 2), indicating that the surface of MMT is slightly primary compared to activated carbon. Additionally, the pHzpc of the composite material (BAC-650-MMT) is 8.6, which shows that the surface properties of the constituent materials are synchronized in the composite material. These findings also suggest that converting carbon into a carbon/clay composite increased the basicity of its surface.

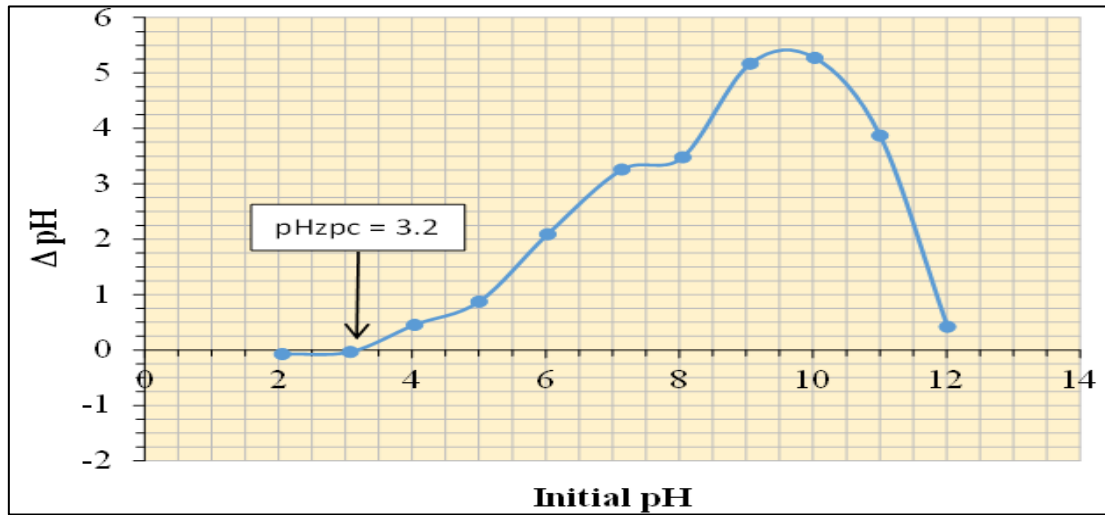


Fig. 2: The pH of point of zero charges (pHzpc) of BENR 2:8.

B. Adsorption of phosphate from aqueous solution

The adsorption of phosphate on all the bentonite samples, modified with various amount of Mg and Fe, were investigated. The results are presented in Figure 3, which shows that without any modification, the bentonite shows very little adsorption (<0.42 mg/g). When bentonite is modified with Fe only, it shows an increase in adsorption to 3.1 mg/g. As the ratio of Mg:Fe increased from 0:10 to 2:8, adsorption gradually increased to 3.47 mg/g. Further increase in ratio to 3:7 shows a sharp loss in adsorption capacity to 2.57 mg/g. On further increase in the ratio to 5:5 a steady increase in adsorption capacity to 3.25 mg/g was

observed. After this ratio, any further increase in Mg in this mixed modification up to 10:0 shows a steady decrease in adsorption capacity of 0.76 mg/g. This batch experiment shows three significant findings; (1) the modification improves the phosphate uptake of bentonite, (2) among single metal modifications Fe (0:10) increases more uptake as compared to Mg (10:0), and (3) the Mg:Fe in 2:8 ratio gives maximum enhancement in terms of phosphate adsorption capacity. Therefore, for further experiments BENR 2:8 was selected for phosphate adsorption from samples.

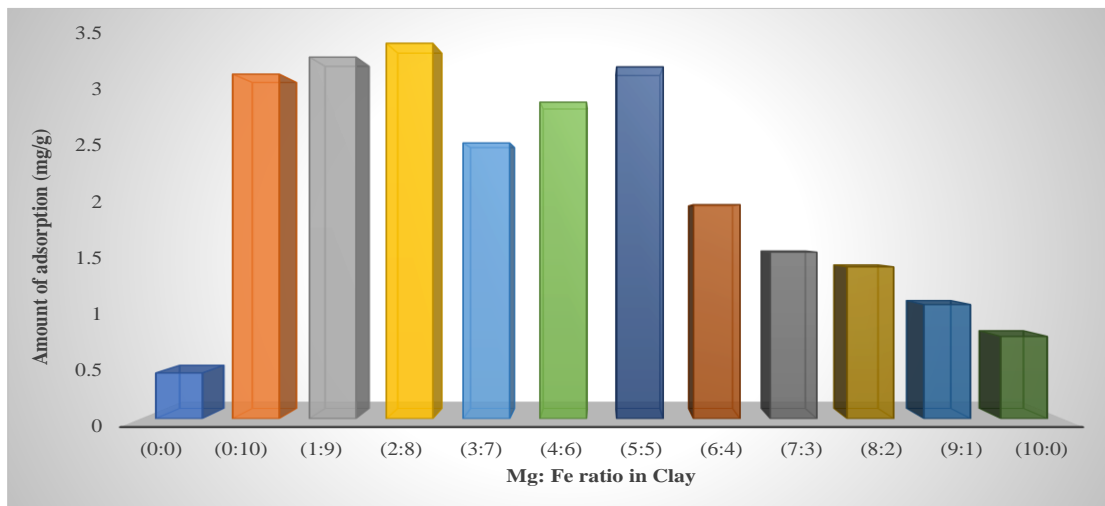


Fig. 3: Effect of Mg:Fe ratio on phosphate uptake capacity of modified bentonite materials.

➤ **Effect of initial concentration and temperature**

The initial phosphate concentration and adsorption temperature an important aspect in terms of adsorption capacity (Zheng et al., 2016). As shown in Figure 4, the effect of initial concentration and temperature on the adsorption of phosphate by the PILC material was studied with 20°C, 30°C, and 40°C. From Fig 3, it could be seen that the adsorption capacity initially increased very rapidly with an increase in initial concentration. After 30 mg/L of initial concentration, the increase in the amount of adsorption

becomes slow, which shows that there are fewer and fewer active sites for adsorption. In the case of the effect of temperature, the adsorption efficiency was slightly enhanced with temperature increasing from 20°C to 40°C, implying that, within a certain range, raising the temperature is conducive to the adsorption process. This may probably be due to the major role of endothermic chemisorption, meanwhile, more phosphate molecules would interact with the active sites in the adsorbent (Amardeep and Melo, 2013).

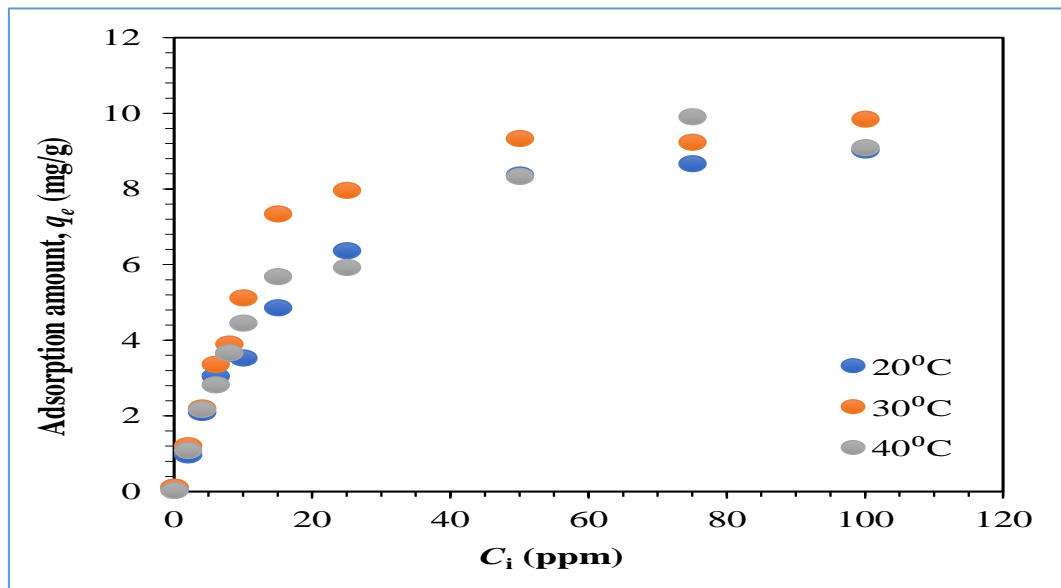


Fig. 4: The effect of initial concentration on uptake of phosphate with BENR 2:8 at different temperatures.

➤ *Effect of contact time on Adsorption*

The effect of contact time optimization was carried out at various intervals between 0 and 1440 minutes with 200mL of 30 mg/L initial concentration of the respective anion at ambient conditions as shown in Figure 5 below. As presented below, the amount of phosphate uptake increases rapidly in the initial 120 minutes, followed by a slow and slight decrease and then an increase in the 360th minute before slightly decreasing again at 540 min before reaching an

equilibrium adsorption state after approximately 180 min. This may conceivably be due to the electrostatic attraction between adsorbent and adsorbate which can lead to rapid adsorption at the initial stage. Moreover, after 120 min, the slight decrease in adsorption capacity may be due to partial desorption of adsorbate. Therefore, all studies were conducted in 1440 min (24h) for optimum outcome since the plot below showed maximum equilibrium adsorption at that time.

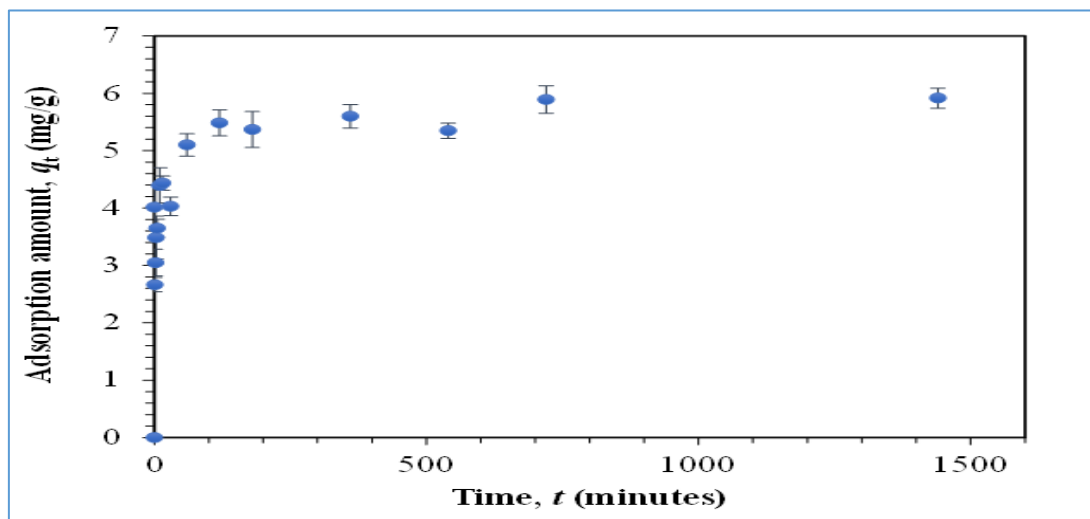


Fig. 5: Effect of contact time on adsorption ($C_i= 30$ mg/L, $T = 20^\circ\text{C}$)

➤ *Effect of solution pH on adsorption*

Generally, one of the important parameters influencing the phosphate adsorption process is the pH value of the solution (Cui et al., 2013). At pH values between 3 and 9, phosphate species are mainly in the form of H_2PO_4^- and HPO_4^{2-} , while the PO_4^{3-} species will dominate upon alkalinity increasing from 9 to 14 (Chen et al., 2009). Phosphate has at least four different species in an aqueous solution, and the concentration varies with the pH of the solution (Figure 6b). The figure below shows the speciation of phosphate in an aqueous solution where at low

pH, it becomes protonated, thus forming orthophosphoric acid, and at high pH, it becomes deprotonated, thus forming phosphate as shown in the Figure below. Also, the Figure shows the individual species in a molecular form. In this study, the effect of pH in the adsorption of phosphate by the prepared PILC Bentonite material was evaluated between pH 1.0 to 14.0. As shown in Figure 6a below, the phosphate solution from pH 4 – 10 behaved as a phosphate buffer in this study. Thus, the effective charge on PO_4^{3-} species at that pH and its possible interaction with the material was related as electrostatic interaction of variable degree.

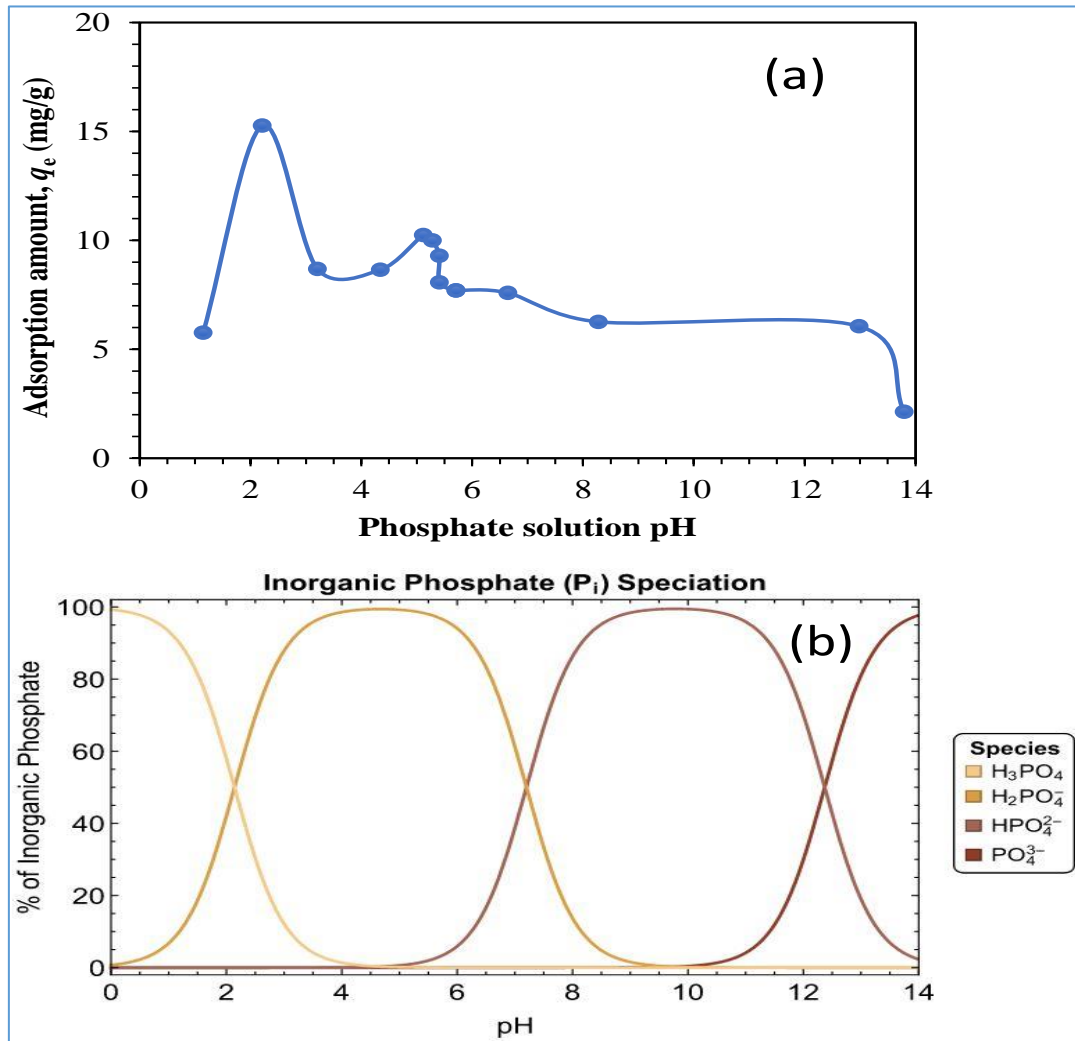


Fig. 6: Effect of solution pH on adsorption (a) and Speciation of phosphate at various pH (b).

Also, the isoelectric charge was studied. During this process, the prepared stock solution pH was initially measured, followed by the bubbling of nitrogen. Different pH values were prepared with the stock solution with the help of HCl and NaOH. The pH_{zpc} value was recorded as 3.2 after the experiment. This implies that when the pH of the solution is less than the pH_{zpc}, then the material becomes positively charged, and when the pH of the solution is greater than the pH_{zpc}, then the material becomes negatively charged. This explains why the maximum adsorption was achieved at pH 2.0 ± 1 .

➤ *Adsorption Kinetics*

The adsorption kinetics data from the effect of contact time (Figure 7) was applied to different kinetic models to analyse the rate of phosphate adsorption on PILC (BENR 2:8). Lagergren and the frequently applied model developed the Pseudo first-order equation. Its equation is,

$$\log(q_e - q_t) = \log q_e - k_1 t \tag{2}$$

Where q_t ($mg \cdot g^{-1}$) and q_e ($mg \cdot g^{-1}$) are the amounts of adsorption on the unit mass of adsorbent at time t (min) and at equilibrium, respectively. The k_1 is the pseudo-first-order

rate constant (min^{-1}). If this model prevails, the plot of $\log(q_e - q_t)$ versus t should give a straight line.

The pseudo-second-order model is written as,

$$\frac{t}{q_t} = \frac{1}{k_2 q_e^2} + \frac{t}{q_e} \tag{3}$$

Where the q_t and q_e have their usual meaning, as mentioned above. The k_2 ($g \cdot mg^{-1} \cdot min$) is the rate constant of the pseudo-second-order model. If this model applies, the plot of t/q_t versus t must give a straight line.

The experimental adsorption kinetic data and the fitting models are illustrated in Figure 8 below. The result of the fittings is presented in Table 1 below. From the figure below, it can be concluded that the Elovich isotherm is the best model to describe the experimental data with its least chi square values. Thus, the rate of adsorption of solute decreases exponentially as the amount of adsorbed solute increases. The table below summarizes the pseudo-first-order model, pseudo-second-order model, and Elovich model using the nonlinear regression method.

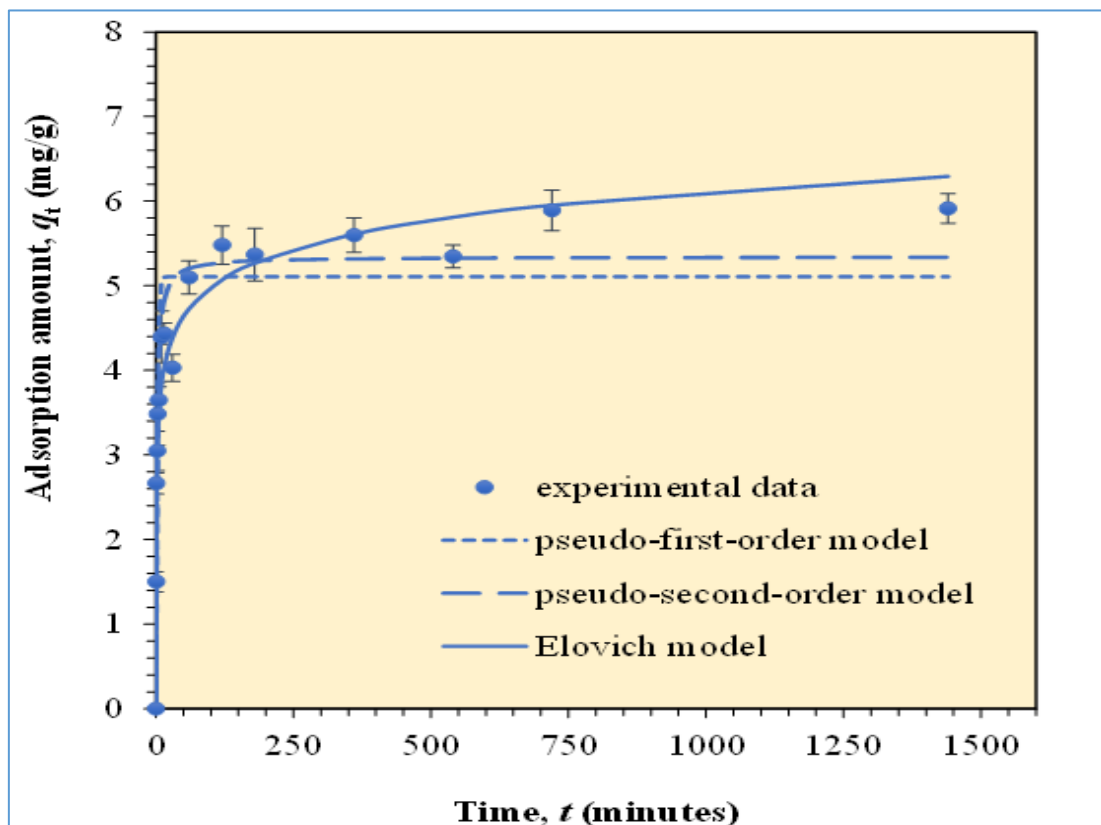


Fig. 7: Adsorption kinetics modeling: fitting of phosphate adsorption data on pseudo-first-order, pseudo-second-order, and Elovich model

The results show that adsorption data did not fit well with the pseudo-first-order model and pseudo-second-order model. Instead, the adsorption data fit well on the Elovich model.

Table 1: Different adsorption models obtained from fitting of adsorption isotherm on three adsorption models.

experimental adsorption capacity q_e (mg·g ⁻¹)		5.91
Adsorption Kinetic Model	Equation and fitting parameters	
Pseudo-first-order	k_1 (min ⁻¹)	0.439
	q_e (mg·g ⁻¹)	5.109
	χ^2	1.576
Pseudo-second-order	k_2 (g·mg ⁻¹ ·min ⁻¹)	0.119
	q_e (mg·g ⁻¹)	5.345
	χ^2	0.6488
Elovich	α (mg·g ⁻¹ ·min ⁻¹)	121.287
	β (g·mg ⁻¹)	2.031
	χ^2	0.615

➤ *Adsorption thermodynamics*

Adsorption isotherm data from experiments were applied to different adsorption models to find the suitability of these models to explain the adsorption mechanism. The fitting of

these model shows that Freundlich model shows better fitting of adsorption isotherm data as compared to Langmuir model, which implies that adsorption of phosphate on BENR 2:8 is multi-layered.

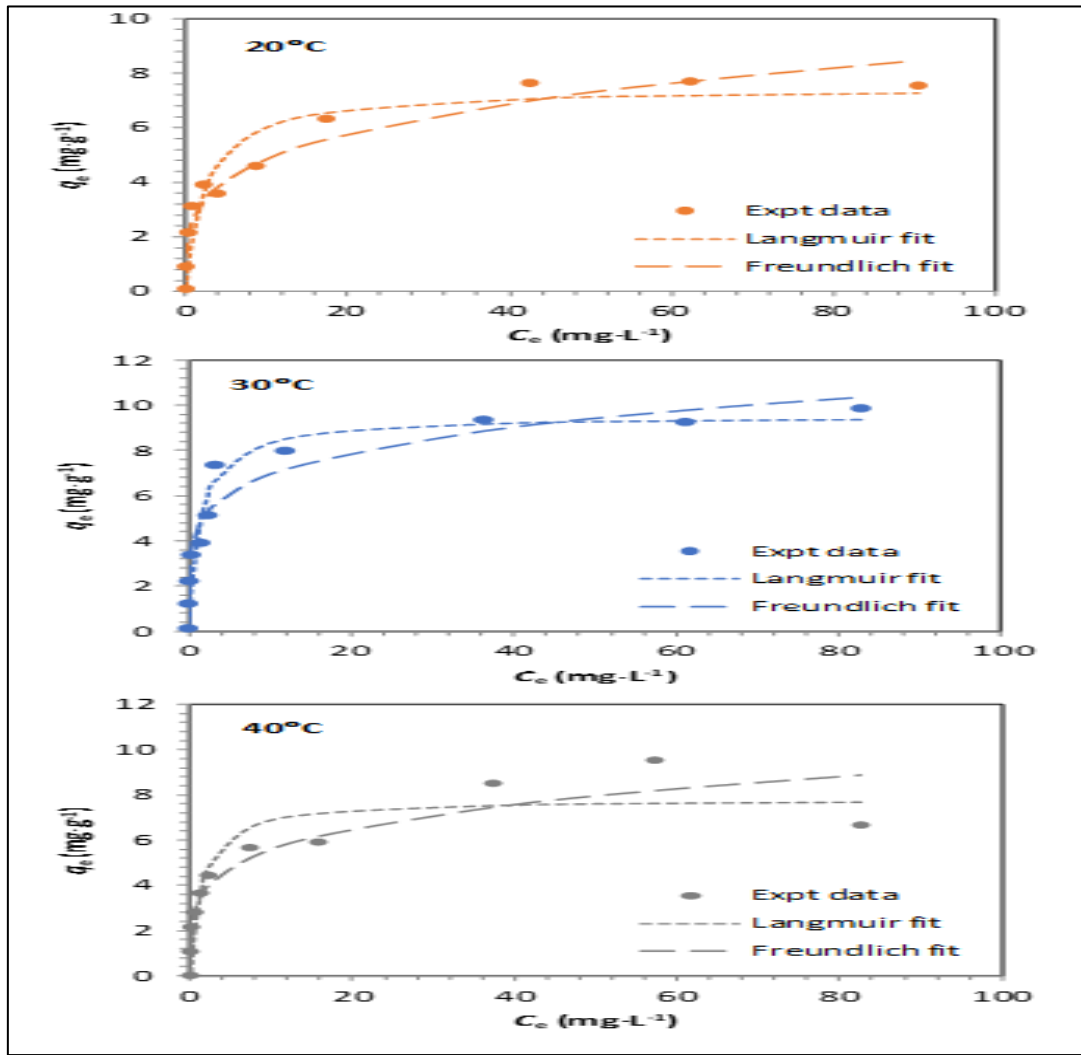


Fig. 8: Fitting of non-linear adsorption isotherm model to adsorption data at different temperatures.

The results of the effect of adsorption temperature on adsorption were applied to different thermodynamic models, to calculate the thermodynamic parameters of the adsorption

process. The vant Hoff plot is presented in the figure below and the resultant thermodynamic parameters are presented in the table below.

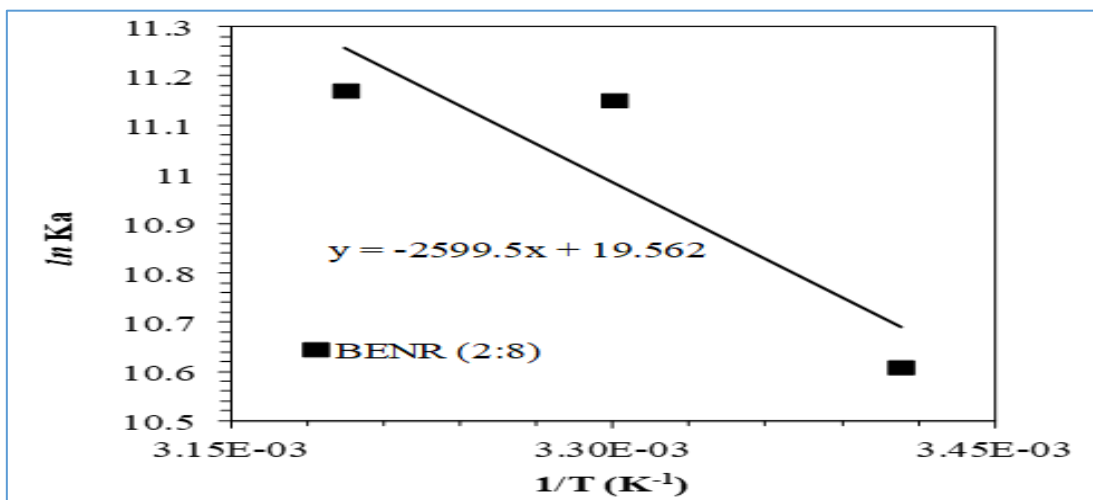


Fig. 9: Vans' Hoff plot for calculation of thermodynamic parameters

The evaluation of thermodynamic parameters (Table 2) shows that change in enthalpy in phosphate adsorption is an endothermic process. The negative values of G show

feasibility of the adsorption process with positive S (entropy) indicating the increase in entropy a adsorbate-adsorbent interface.

Table 2: Thermodynamic parameters of adsorption with selected material

Sample	Temp (K)	A (L·mg ⁻¹)	K _a (L·mol ⁻¹)	ΔG° (kJ·mol ⁻¹)	ΔH° (kJ·mol ⁻¹)	ΔS° (J·mol ⁻¹ ·K ⁻¹)
BENR (2:8)	293	0.409	40482.53	-25.84	21.61	162.63
	303	0.703	69582.45	-28.09		
	313	0.717	70968.16	-29.07		

C. Recovery from fresh urine

➤ Human Urine

The human urine of a 25-year-old male was collected for a 24 h duration. The total volume of the urine sample was 3100 mL (in 24h). The pH of the sample was recorded as 6.38 and the phosphate content in the urine was recorded as 92.11 mg/L. The extent of adsorption from urine and recovery of phosphate from adsorbed samples under natural and acidified conditions are presented in Figure 10. From the figure below, the different pH shows similar phosphate recovery capacities. That is, the natural urine of pH 6.38 had a recovery capacity of 10.144 mg/g implying 22.03% of

adsorption. Similarly, the acidified urine with a pH value of 2.0 had a recovery capacity of 9.607mg/g implying 21.43% of adsorption.

After the recovery of phosphate from the fresh urine, the PILC material (BENR 2:8) with adsorbed phosphate was separated from the urine sample by centrifuging and oven drying at 60°C. The adsorbed phosphate was then desorbed using a NaOH solution of 2N, which was used as a desorption agent because a high molarity of NaOH influenced phosphate desorption to a great degree as describe in the figure below.

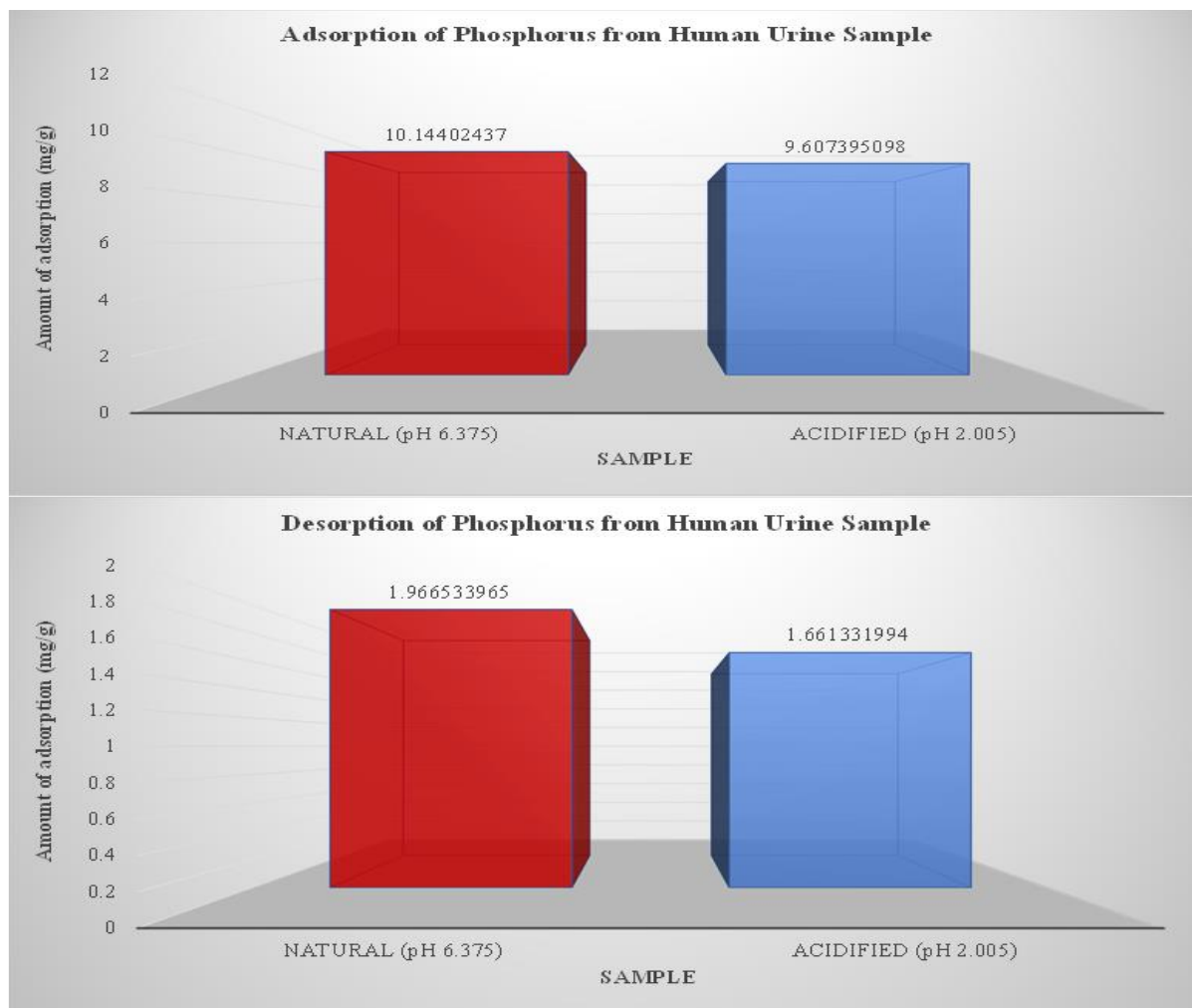


Fig. 10: The adsorption and desorption of phosphate from human urine under natural and acidified conditions.

As shown in the above figure, the desorption capacity of the Natural urine sample was recorded at 1.967 mg/g which signifies a desorption efficiency of 11.066%. Also, the Acidified urine sample recorded a desorption capacity of 1.661 mg/g, implying 9.27% desorption efficiency.

➤ *Recovery from Cow Urine*

The same procedure was duly followed for the recovery of phosphate from cow urine as in human urine. The total volume of the sample was 1400 mL (a one-time sample collection). The pH value of the sample recorded was 8.030 and the phosphate concentration in the sample was recorded as 2.05 mg/L. The recovery of phosphorus in the Natural

urine sample with a pH value of 8.03 recorded 0.433 mg/g which signifies 42.09% of adsorption as compared to the acidified sample of pH 2.014 recording 0.052 mg/g, implying 5.05% of adsorption (Figure 11).

Also, the desorption of phosphorus in cow urine was studied in the same procedure as in that of the human urine. As shown below, the desorption capacity of the Natural urine sample recorded 0.295 mg/g which signify a desorption efficiency of 99.65% as compared to the Acidified urine sample recorded a desorption capacity of 0.362 mg/g, implying 74.88% desorption efficiency.

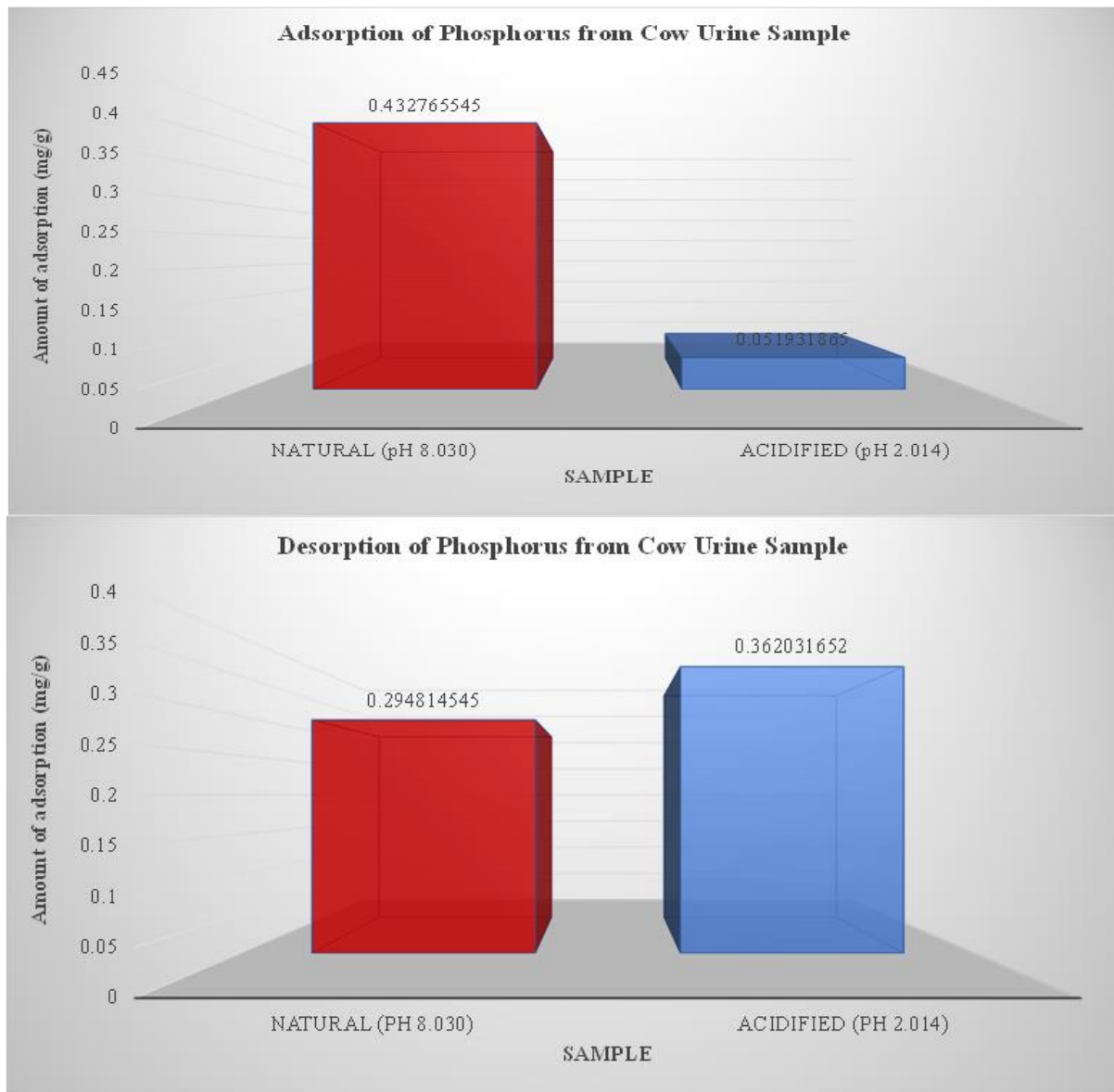


Fig. 11: The adsorption and desorption of phosphate from cow urine under natural and acidified conditions.

However, it could be seen that the desorption phosphorus value for the Acidified cow urine sample is more than the adsorbed phosphorus value. This is quite unrealistic because desorption is the inverse of adsorption, hence desorption value cannot be more than the adsorption value. This may be due to a number of factors such as since the concentration of phosphate in the urine sample was minimal, the margin of error becomes high. Also, the urine

sample was just a one-time sample since the 24 h collection was inconvenient.

Therefore, the adsorption and desorption experiment on the Cow urine sample was considered inconclusive.

IV. CONCLUSION

The finding of this study indicates a promising way to recover phosphate using a locally available Bentonite, which would help promote sustainability. Basic conditions such as temperature, contact time, and pH markedly influence the adsorption of phosphorus in both aqueous and real urine samples. Elovich isotherm model was the best-fit model in this study. Therefore, this study concludes that Bentonite clay is a suitable material for phosphate recovery from urine samples. The concentration of Mg/Fe in a 2:8 ratio is the most suitable ratio to achieve maximum recovery of phosphate from an aqueous as well as real urine samples. The acidic solution of phosphate offers high adsorption on prepared material. The adsorbed phosphate can be efficiently recovered with a 2.0 N NaOH solution. The selectivity and adsorption capacity of prepared material was higher with human urine as compared to aqueous solution of similar concentration. Finally, the adsorption and desorption of phosphate on Cow urine was deemed inconclusive since the concentration of phosphate in the cow urine sample was very low due to the fact that the 24 h urine sample couldn't be collected due to practical problems.

ACKNOWLEDGEMENTS

The Authors acknowledge the help and support of the University Grant Commission (UGC), New Delhi, India, for financial support under the MRP scheme (Project No.: MRP-MAJOR-ENVI-2013-35206). Michael Biney would like to acknowledge the help from Dr. Vandana Yadav and Doon University, Dehradun for essential research infrastructure.

REFERENCES

- [1]. Brian Oram. Wilkes University Center for Environmental Quality, GeoEnvironmental Sciences and Engineering Department, Phosphate and Water Quality Available @ <http://www.water.research.net/watershed>, 2005.
- [2]. Cheng, X., Huang, X., Wang, X., Zhao, B., Chen, A., Sun, D., 2009. Phosphate adsorption from sewage sludge filtrate using zinc-aluminum layered double hydroxides. *J. Hazard Mater.* 169 (1–3), 958–964.
- [3]. Cordell, D., Drangert, J.-O., White, S., 2009. The story of phosphorus: global food security and food for thought. *Glob. Environ. Chang.* 19, 292–305.
- [4]. Emsley, J. 1980. The phosphorus cycle. In *The handbook of environmental chemistry: The natural environment and the biogeochemical cycles*, edited by O. Hutzinger, p. 147–167. New York: Springer-Verlag Berlin Heidelberg.
- [5]. Emsley, J. 2000. *The shocking history of phosphorus*. London: Macmillan
- [6]. Farmer, A.M., 2018. Phosphate pollution: A global overview of the problem. In: Schaum, C. (Ed.), *Phosphorus: Polluter and Resource of the Future – Removal and Recovery from Wastewater*. IWA Publishing.
- [7]. Filippelli, G. M. 2002. The global phosphorus cycle. *Reviews in Mineralogy and Geochemistry* 48: 391–425.
- [8]. Follmi, K. B. 1996. The phosphorus cycle, phosphogenesis and marine phosphate-rich deposits. *Earth-Science Reviews* 40(1–2): 55–124.
- [9]. Genz, A., Kornmuller, A., Jekel, M., 2004. Advanced phosphorus removal from membrane filtrates by adsorption on activated aluminium oxide and granulated ferric hydroxide. *Water Res.* 38, 3523–3530.
- [10]. Grove, T. L. 1992. Phosphorus, biogeochemistry. In *Encyclopedia of earth system science*, edited by W. A. Nierenberg, p. 579–587. London: Academic Press.
- [11]. Manahan, S.E.; *Fundamentals of Environmental Chemistry*, Lewis Publishers: London; 1993; p 504.
- [12]. Metcalf & Eddy, Inc. 2003. *Wastewater engineering: treatment and reuse*. Boston :McGraw-Hill
- [13]. Meybeck, M. 1982. Carbon, nitrogen, and phosphorus transport by World Rivers. *American Journal of Science* 282(4): 401–450.
- [14]. Mueller, D.K.; Hamilton, P.A.; Helsel, D.R.; Hitt, K.J.; Ruddy, B.C. *US Geological Survey Water Resources Investigations Report 95-4031*, Denver, Colorado, 1995.
- [15]. Richey, J. E. 1983. The phosphorus cycle. In *The major biogeochemical cycles and their interactions*, edited by B. Bolin and R. B. Cook, p. 51–56. New York: Wiley.
- [16]. Schlesinger, W. H. 1991. *Biogeochemistry: An analysis of global change*. San Diego, CA: Academic Press.
- [17]. Sheila Murphy, *USGS Water Quality Monitoring*, available at <http://www.water.usgs.gov/nawqa/circ-1136.html>; 2005.
- [18]. Sprail, T.B.; Harned, D.A.; Ruhl, P.M.; Eimers, J.L.; McMahan, G.; Smith, K.F.; Galeone, D.R.; Woodside, M.D. U.S. Geological Survey Circular 1157; online at URL:<http://water.usgs.gov/pubs/circ.1157>; 1998.
- [19]. Su, Y., Cui, H., Li, Q., Gao, S., Shang, J.K., 2013. Strong adsorption of phosphate by amorphous zirconium oxide nanoparticles. *Water Res.* 47 (14), 5018–5026.
- [20]. Villalba, G., Y. Liu, H. Schroder, and R. U. Ayres. 2008. Global phosphorus flows in the industrial economy from a production perspective. *Journal of Industrial Ecology*, in press.